

# BRIEF: Backward Reduction of CNNs with Information Flow Analysis

Yu-Hsun Lin  
HTC Research & Healthcare  
lyman\_lin@htc.com

Chun-Nan Chou  
HTC Research & Healthcare  
jason.cn\_chou@htc.com

Edward Y. Chang  
HTC Research & Healthcare  
edward\_chang@htc.com

**Abstract**—This paper proposes BRIEF, a backward reduction algorithm that explores compact CNN-model designs from the information flow perspective. This algorithm can remove substantial non-zero weighting parameters (redundant neural channels) of a network by considering its dynamic behavior, which traditional model-compaction techniques cannot achieve. With the aid of our proposed algorithm, we achieve significant model reduction on ResNet-34 in the ImageNet scale (32.3% reduction), which is 3× better than the previous result (10.8%). Even for highly optimized models such as SqueezeNet and MobileNet, we can achieve additional 10.81% and 37.56% reduction, respectively, with negligible performance degradation.

**Index Terms**—CNN, Deep Learning, Model Reduction

## I. INTRODUCTION

Since the breakthrough performance demonstrated by convolutional neural networks (CNNs) on ImageNet, deep architecture has been successfully applied to a number of areas such as speech recognition, object tracking, and image classification. As the width and depth of a CNN is increased to improve prediction accuracy, the model complexity and training time increase as well. Whereas model training can be sped up by employing a large number of GPUs, inferencing on mobile and wearable devices (e.g., mobile VR) faces the resource limitations of memory, power and computation. In this work, we utilize information flow analysis to perform CNN model reduction while preserving prediction accuracy.

Traditionally, a complex CNN is simplified for embedded systems by using the *teacher-student* model [1], [2]. Such simplification demonstrates that important properties of a CNN can be preserved when its model complexity is reduced. However, almost all model-reduction approaches treat a CNN as a black-box and simply compress the model parameters obtained by the training process. Much effort has recently been devoted to opening the black-box to better understand and interpret CNNs. The work by [3] proposes the use of information theory to analyze the internal behaviors of a deep architecture. Inspired by this approach, our work incorporates information density to conduct model reduction. Our information-based approach works orthogonally to the traditional black-box approach (discussed further in Section II), and can achieve additional compaction while preserving prediction accuracy.

We first conduct lesion studies to probe the dynamic nature of the network robustness in CNNs with the information density consideration. We define *convolution macroblock* as

the set of convolution layers whose output feature maps have the same height and width. Our lesion studies provide important clues for us to construct a hypothetical information flow structure. The hypothetical structure is useful for guiding us to design an effective model reduction algorithm. The hypothetical framework formulates a CNN as an information pipeline consisting of cascaded convolution macroblocks. Our aim is to identify the fewest channel numbers<sup>1</sup> with sufficient information flow between macroblocks so as to reduce their associated parameters. We propose our *backward reduction* algorithm named BRIEF, which incorporates the hypothetical information flow structure to achieve our twin design goals of model reduction and accuracy preservation.

The contributions of this work can be summarized as follows:

- *Applicable to various CNN models.* We propose an information-based model reduction algorithm, *backward reduction*, which can be applied to any already compact CNN structures such as MobileNet [4], ResNet [5], and SqueezeNet [6] to achieve further model-size reduction.
- *Significant reduction results.* With the aid of BRIEF, we are able to compress MobileNet to a model size that is smaller than that of SqueezeNet while achieving higher prediction accuracy. We also achieve a 32.3% model reduction on ResNet-34 with ImageNet, which is 3× better than the state-of-the-art approach (10.8%) presented in [7]. Even in the case of SqueezeNet, a highly optimized model, we can achieve additional 10.8% reduction with negligible prediction degradation.
- *Further model compaction.* The Convolution-layer dominant models are inherently compact and become the default choices for mobile devices. Our proposed framework can further shrink these highly optimized CNN models (e.g., MobileNet [4]). Most traditional compaction works regard the CNN as a black-box and perform either parameter elimination or compression within a limited range. Our method utilizes the distribution trends of the information density and the dynamic nature of CNNs, which works orthogonally to the black-box approach. Therefore, we can reduce the model size of CNNs further.

<sup>1</sup>The input to a convolution layer is a set of input tensors, each of which is called a channel [13].

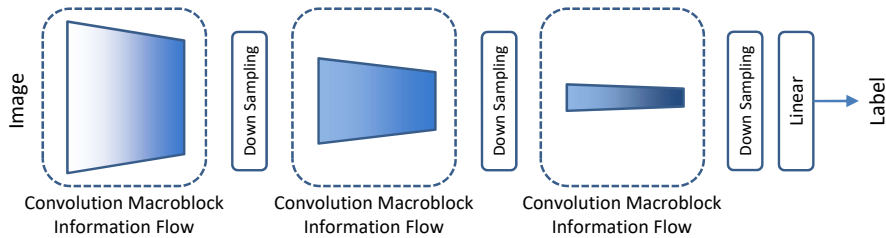


Fig. 1. (a)The information flow structure conjectured from the the DPI theorem. The information density within the information flow is in a descending trend for each convolution macroblock. A macroblock represents the set of convolution layers whose the output feature maps have the same height and width.

To the best of our knowledge, this is the first work to achieve significant reduction on already highly compact CNN models using information flow analysis. The remainder of this paper is organized into four sections. Section II describes related work in CNN models and model-reduction techniques. Section III explains our hypothetical information flow structure and presents our proposed backward reduction algorithm. Section IV details experiments. We offer our concluding remarks in Section V.

## II. RELATED WORK

The rapid increase of the number of parameters from the cascaded fully connected (FC) layers is the main reason for excessive CNN model size. Recent developed CNN models (e.g., ResNet [5], DenseNet [8], and MobileNet [4]) show that with the aid of improved structural design, the cascaded FC layer design is not mandatory for achieving high prediction accuracy. These improved designs include, but are not limited to, batch normalization [9] and bottleneck structure [10]. Though these new models without many cascaded FC layers are highly compact, we propose BRIEF from the information density perspective to further compact these models.

This section first reviews existing CNN models (Section II-A) and then traditional black-box model-reduction approaches (Section II-B). In comparison with the traditional methods, our BRIEF is a coarse-grained model compaction technique applicable to both FC-layer dominant and Convolution-layer dominant CNN models.

### A. Categories of CNNs

A CNN typically consists of convolutional layers, pooling layers, and FC layers. Based on the distribution of the model parameters in a CNN, we can categorize the CNN as either FC-layer dominant or Convolution-layer dominant.

- *FC-layer dominant models.* A model is considered as FC-layer dominant when the parameters of FC layers comprise more than 50% of the total parameters in a CNN. The well-known AlexNet [11] and VGGNet [12] models are examples of FC-layer dominant CNNs. CNNs in this category usually possess huge model footprints that are mainly contributed by the parameters of the FC layers. The parameters of the FC layers in VGG-11 account for 472MB (93%) out of the total 507MB storage.

- *Convolution-layer dominant models.* The recent trend of CNNs replaces the cascaded FC layers with a global average pooling layer. The parameters of FC layers now comprise less than 20% of parameters in the whole model. CNNs in this category are compact models with high prediction accuracy. For example, MobileNet takes up only 16.25MB of storage but possesses VGG-level accuracy.

### B. Model Reduction Techniques

Based on the level of involved structures, the model reduction techniques can be classified into two categories: fine-grained and coarse-grained [13].

- *Fine-grained approaches.* There are various reduction techniques applied on the filter/kernel level. Such techniques include sparse convolution [14] and deep compression [15]. The irregular structures introduced on the filter/kernel level often require special hardware acceleration [16]. Replacing the cascading FC layers with an average pooling layer introduces negligible performance degradation. FC layer pruning [17] usually achieves significant reduction since FC layers are sparse in nature. Binary filter/kernel approximation methods are also popular algorithms to model reduction [18]–[21]. However, retaining the prediction accuracy of a binary CNN is a challenging issue. This issue is addressed and relaxed by using multiple binary representations [22], [23].
- *Coarse-grained approaches.* The coarse-grained techniques conduct filter pruning [7], [24], [25], which removes irrelevant filters/kernels from the model. The filter importance is determined by filter weight magnitude [7] or derived from the similarity among inter-layer feature maps [25]. The work of [24] integrates an additional scaling factor for each filter output during the training process, which the magnitude of the factor reflects the filter importance. Conducting pruning at the filter-level can free us from designing kernel-specific hardware/software solutions.

## III. METHOD

In this section, we study the information flow of CNNs using the data processing inequality of information theory [27]. We investigate the relationship between the network robustness and the information density of CNNs by our designed lesion

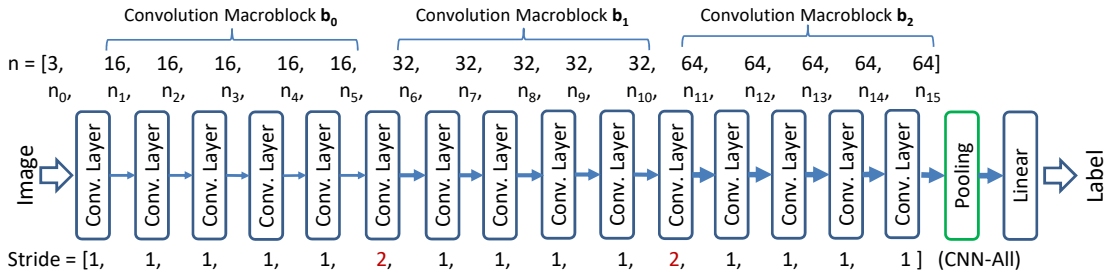


Fig. 2. A sequential CNN example where the convolution depth = 15. Each layer is composed of Conv-BN-Relu modules.

studies. Our lesion studies reveal the dynamic nature of the network robustness of CNNs for dealing with the distortions caused by channel removal. We utilize the insights observed from our lesion studies to later (in Section III-D) propose our backward model-reduction algorithm.

### A. Descending Trend of Information Density

The data processing inequality (DPI) theorem [27] shows that for the variables forming a Markov chain  $X \rightarrow X' \rightarrow Y$ , we have

$$I(X; X') \geq I(X; Y), \quad (1)$$

where  $I(X; Y)$  represents the mutual information between variables  $X$  and  $Y$ .

Let us consider a CNN as an information pipeline where its input is images and post-processing operations are convolution and filtering. Based on the DPI theorem, the information density in the CNN information pipeline must exhibit a decreasing trend. This information decreasing trend can also explain the phenomenon observed by [13] that the activation outputs of the latter layers of a CNN are increasingly sparse. We plot Figure 1 to illustrate our theoretically justified conjecture that the latter macroblocks (defined in Section I) of a CNN contain lower information density than the earlier ones. This conjecture establishes the foundation of our model-reduction scheme.

### B. Lesion Study: Definitions and Setup

How can the trend of decreasing information density help reduce the model size of a CNN? This section conducts lesion studies to shed the insights. Our lesion consists of three components: the CIFAR-10 dataset, a sequential CNN, and our designed one-hot lesion:

**CIFAR-10 Dataset.** CIFAR-10 consists of natural images with resolution  $32 \times 32$  of 10 classes, and divides 50k images for training and 10k images for testing. CIFAR-10 is not too large (convenient for us to run many experiments) and contains sufficient natural images to reflect CNN behaviors. The network on CIFAR-10 was trained using SGD, weight decay  $10^{-4}$ , momentum 0.9, and mini-batch size 128. Following the work of [5], we set the initial learning rate to be 0.1 and divided by 10 at 50% and 75% of the total epochs, respectively.

**Sequential CNN.** The sequential CNN consists of the VGG-like structure where the cascaded FC layers are replaced by

a global average pooling layer and an FC layer in order to simulate a convolution-layer dominant CNN. This model serves as our reference model because of its simplicity and representative structures. In particular, the “down-sampling then  $2 \times$  channel number” design is widely adopted in modern compact CNN models (e.g., MobileNet [4]) for considering the trade-off between model complexity (e.g., size) and prediction accuracy.

Figure 2 shows an example of sequential CNNs, which has 15 convolution layers. The notation  $n_i$  ( $i \geq 1$ ) represents the number of the output channels of convolution layer  $L_i$ . We define  $n_0$  as the channel number of input images and use the following vector to represent the channels in the sequential CNN,

$$\mathbf{n} = [n_0, n_1, \dots, n_N], \forall n_i \in \mathbb{N}. \quad (2)$$

The channels that have the same size of output feature maps are grouped into the same *convolution macroblock*  $b_i$ . For example, the channels  $[n_1, \dots, n_5]$  ( $n_0$  is not an output channel number) in Figure 2 are grouped into macroblock  $b_0$ . The configuration  $\mathbf{n}_b$  of macroblocks of a sequential CNN model is denoted by  $\mathbf{n}_b = [n_{b_0}, \dots, n_{b_m}]$  such as  $\mathbf{n}_b = [16, 32, 64]$  for the model in Figure 2.

**One-hot Lesion.** We analyze the alteration in the prediction accuracy of our sequential CNN models by constant and proportional one-hot lesions, depicted as follows:

- Constant one-hot lesion. For each individual lesion experiment, we set  $n_i = c$  for only one selected index  $i$  and keep the other channel numbers  $n_j$  ( $j \neq i$ ) unchanged. This constant one-hot lesion is denoted as  $h_i(\mathbf{n}, c)$ .
- Proportional one-hot lesion. For each individual lesion experiment, we set  $n_i = k \times n_i$  for only one selected index  $i$  and keep the other channel numbers  $n_j$  ( $j \neq i$ ) unchanged. Parameter  $k$  is tunable. This proportional one-hot lesion is denoted as  $h_i(\mathbf{n}, k \times n_i)$ .

Table I illustrates an example of a one-hot lesion for a sequential CNN with convolution depth 15.

We conduct a one-hot lesion (between convolution layers) first to investigate the prediction accuracy behaviors at the channel level of a sequential CNN model. We then investigate at the macroblock level about rate distortion (RD) performance, which is an important criterion in lossy compression from the perspective of information theory.

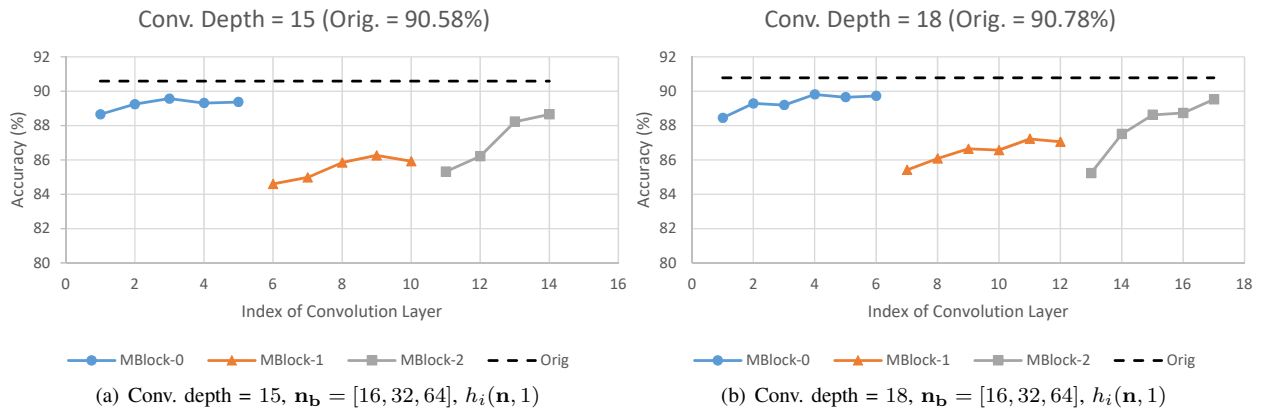


Fig. 3. Each point represents a lesion experiment of a one-hot lesion vector  $h_i(\mathbf{n}, 1)$ . The dashed black line represents the original prediction accuracies that are (a) 90.58% and (b) 90.78%.

TABLE I  
AN EXAMPLE OF CONSTANT ONE-HOT LESION  $h_i(\mathbf{n}, c)$  AND  
PROPORTIONAL ONE-HOT LESION  $h_i(\mathbf{n}, k \times n_i)$  FOR THE SEQUENTIAL  
CNN WITH CONVOLUTION DEPTH = 15

Lesion	Channel Width (Conv. Depth=15)
Constant	
$\mathbf{n}$	[3, 16, 16, 16, 16, 16, 32, 32, 32, 32, 32, 64, 64, 64, 64, 64]
$h_1(\mathbf{n}, c)$	[3, c, 16, 16, 16, 16, 32, 32, 32, 32, 32, 64, 64, 64, 64, 64]
$\dots$	$\dots$
$h_{14}(\mathbf{n}, c)$	[3, 16, 16, 16, 16, 16, 32, 32, 32, 32, 32, 64, 64, 64, c, 64]
Proportional	
$\mathbf{n}$	[3, 16, 16, 16, 16, 16, 32, 32, 32, 32, 32, 64, 64, 64, 64, 64]
$h_1(\mathbf{n}, kn_1)$	[3, $kn_1$ , 16, 16, 16, 16, 32, 32, 32, 32, 32, 64, 64, 64, 64, 64]
$\dots$	$\dots$
$h_{14}(\mathbf{n}, kn_{14})$	[3, 16, 16, 16, 16, 16, 32, 32, 32, 32, 32, 64, 64, 64, $kn_{14}$ , 64]

### C. Lesion Study: Analysis

Our experiments aim to find the relationship between model size and model prediction accuracy at different levels: first at the channel level and then at the macroblock level.

In constant one-hot lesion at the channel level, we expected that keeping only a constant  $c$  channel number in the latter macroblocks would suffer from severer degradation in prediction accuracy. This expectation is based on the fact that the channels in the latter macroblocks are much wider, and constant one-hot lesion takes more information away from the channels in the latter macroblocks (e.g., keeping  $c$  out of 64) than from the earlier ones (e.g., keeping  $c$  out of 32). Figure 3 plots the result of constant one-hot lesion at the channel level. The x-axis denotes the selected channel index  $i$  for  $h_i(\mathbf{n}, c)$ . The y-axis shows the corresponding prediction accuracy of the modified CNN on CIFAR-10. Surprisingly, macroblock  $b_2$  enjoys an unexpected accuracy *bounce*: the accuracy achieved by removing more channels from macroblock  $b_2$  is higher than the accuracy achieved by removing less channels from  $b_1$ .

Figure 4 plots the experimental results of proportional one-hot lesion. Why did we perform this study? Constant one-

hot lesion keeps only one channel (or  $c$  channels) alive in each macroblock. One may argue that such an extreme study may have more severely penalized the later macroblocks with larger number of channels being removed. Thus, we conduct proportional one-hot lesion to keep alive the same percentage of channels in all macroblocks. In the first experiment we set the alive channels to be one sixteenth, and the second experiment one eighth. Figures 4(a) and 4(b) show that when one sixteenth channels are kept, the *bounced* behavior on macroblock  $b_2$  still exhibits. Since we increase the channel number of proportional one-hot lesion, the prediction accuracy gap is reduced between macroblocks  $b_1$  and  $b_2$ . When we further increase the alive channels to one eighth, Figures 4(c) and 4(d) show that the distortion of all one-hot lesion is limited (i.e.,  $\leq 2\%$  accuracy drop). The *bounced* behavior still exists though less significant. Figure 4(d) illustrates that macroblock  $b_2$  has the highest average prediction accuracy among all macroblocks.

These two lesion studies demonstrate that macroblock  $b_2$  provides better accuracy recovery as compared with macroblock  $b_1$  even though we remove much more channels from  $b_2$  in both constant and proportional one-hot lesion studies. Two observations can be made from these two studies. First, CNN is robust for information-loss recovery. Second, the channels in the latter macroblocks seem to have higher degrees of information redundancy.

We next extend proportional one-hot lesion to the macroblock level to investigate the relation between model size and prediction accuracy. Let  $h_i(\mathbf{n}_b, k \times n_{b_i})$  denote channel number reduction in the macroblock level, which we reduce all channels in macroblock  $b_i$  from  $n_{b_i}$  to  $k \times n_{b_i}$  ( $0 < k < 1$ ) and keep the other channels in  $b_j$  ( $j \neq i$ ) intact.

Figure 5 shows the RD performance of each macroblock by  $h_i(\mathbf{n}_b, k \times n_{b_i})$ , where  $k = [\frac{11}{16}, \dots, \frac{15}{16}]$ . The x-axis depicts the model size of the reduced CNN model from small on the left-hand side to large on the right-hand side. The y-axis depicts the corresponding prediction accuracy of the modified CNN trained on CIFAR-10. Figure 5 shows that macroblock

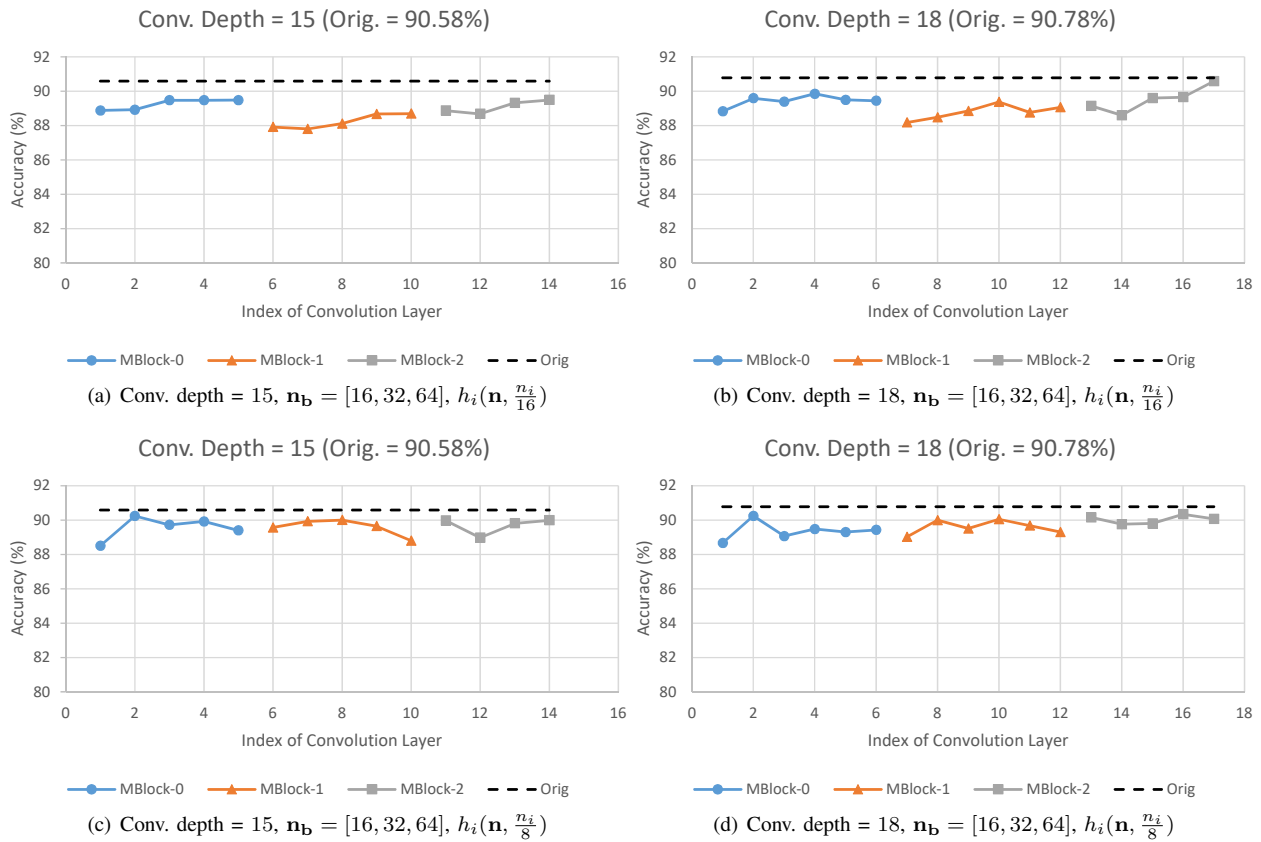


Fig. 4. Each point represents a lesion experiment of a proportional one-hot lesion vector. The configuration [conv. depth, one-hot lesion] for each lesion study is (a) [15,  $h_i(\mathbf{n}, \frac{n_i}{16})$ ], (b) [18,  $h_i(\mathbf{n}, \frac{n_i}{16})$ ], (c) [15,  $h_i(\mathbf{n}, \frac{n_i}{8})$ ] and (d) [18,  $h_i(\mathbf{n}, \frac{n_i}{8})$ ].

$b_2$  (in gray) enjoys the best RD performance (by maintaining high prediction accuracy) among the macroblocks. In addition, macroblock  $b_2$  enjoys the best compaction since the model size is significantly reduced by compressing macroblock  $b_2$  as compared with compacting the other macroblocks.

These lesion studies lead to our following hypotheses:

- *The latter macroblock contains lower information density.* We can observe that the latter macroblock has lower information density based on our lesion studies. The last macroblock  $b_2$  has better prediction accuracy even after we have removed more channels from it than from macroblock  $b_1$ .
- *Network distortion is based on information density.* The actual network distortion is correlated with the information density instead of simply the number of removed channels. Therefore, the network demonstrates strong capabilities to recover from the distortions when we remove the channels with low information density.

#### D. Backward Reduction for Model Reduction

Figure 6 describes the key idea of our proposed backward reduction method. The down-sampling layer plays the role of being an information gateway, through which information (some may be redundant) passes for achieving  $q\%$  prediction accuracy. We can reduce the information flow by decreasing

the channel number of the previous convolution macroblock as long as there maintains sufficient information for achieving the target accuracy. While applying this idea recursively, we must ensure the information to be still sufficient for the classification task in the FC-Layer. Since the classification is performed at the end of a CNN pipeline, our model reduction process starts from the last convolution macroblock. Another reason to perform backward instead of forward reduction is that our lesion studies reveal the latter macroblocks containing lower information density. We will shortly justify this backward choice by presenting experimental results.

Algorithm 1 presents our proposed *backward reduction* algorithm (named BRIEF) based on the information flow structure conjectured from a combination of information flow density and the dynamic nature of CNNs.

The model reduction problem of a CNN can be formulated as follows

$$\min_{\mathbf{n}'} R(\mathbf{n}'), \text{ subject to } D(\mathbf{n}', \mathbf{n}) \leq \delta, \quad (3)$$

where  $R(\mathbf{n}')$  represents the bit rate of the model for the optimized channel width configuration  $\mathbf{n}'$ ,  $D(\mathbf{n}', \mathbf{n})$  denotes the prediction accuracy degradation as compared with the original performance, and  $\delta$  is the acceptable performance loss budget.

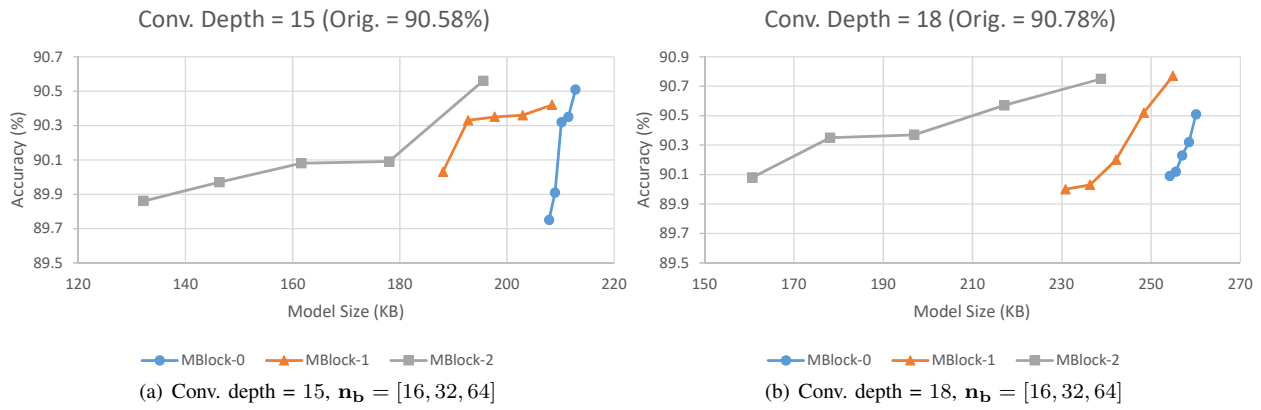


Fig. 5. RD curve of each macroblock for  $h_i(\mathbf{n}_b, kn_{b_i})$ , where  $k = [\frac{11}{16}, \dots, \frac{15}{16}]$ .

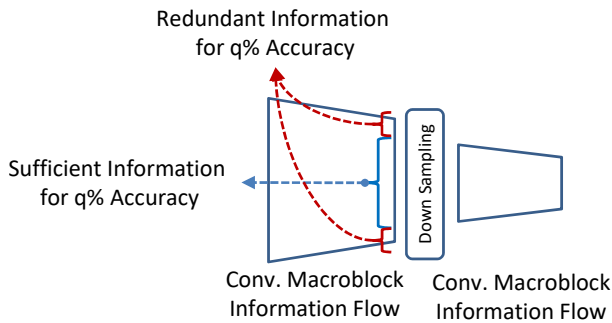


Fig. 6. A conceptual illustration of the proposed backward reduction method that is based on the conjectured information flow structure.

The model reduction formulation of Eq. (3) encapsulates an integer programming problem (i.e., channel number  $n_i$ 's must be positive integers), which makes the optimization an NP-hard problem. Furthermore, no closed-form distortion evaluation function exists, since the CNN is usually considered to be a black-box. Fortunately, with the aid of the conjectured information flow structure, we can reduce the original NP-hard problem to solving a one-dimensional greedy search problem. We search for the proper scaling factor  $\beta_i$  starting from the last convolution macroblock,

$$\min_{\beta_i} n'_{b_i} = \lceil \beta_i n_{b_i} \rceil, \text{ subject to } D(\mathbf{n}, \mathbf{n}') \leq \delta. \quad (4)$$

That is, we optimize for the proper value of the scaling factor  $\beta_m$  for the last convolution macroblock  $b_m$  within distortion budget  $\delta$ . Then we iterate through the same greedy search process for the previous convolution macroblock  $b_{m-1}$ .

Our algorithm optimizes for the channel width multiplier  $\beta_i$  for each convolution macroblock from  $b_m$  down to  $b_0$ . The initial setting of the lower bound  $L = 0.5$  in step 2 is based on the observation by MobileNet [4] that there is a significant drop in prediction accuracy when the channel multiplier is less than 0.5. The default distortion budget  $\delta$  in our algorithm is set to 1%.

---

### Algorithm 1 Backward Reduction

---

**Input:**  $[b_0, \dots, b_m]$  and  $\delta$   
*/\**  $[b_0, \dots, b_m]$ : Convolution macroblocks  
*/\**  $\delta$ : Threshold of accuracy distortion  
**Output:**  $\beta = [\beta_0, \beta_1, \dots, \beta_m]$   
*/\**  $\beta$ : Macroblock-wise Channel Width Multipliers

- 1: **for** macroblock  $b_i := b_m$  to  $b_0$  **do**
- 2:    $U = 1, L = 0.5$
- 3:   **while**  $[(U - L)n_{b_i}] > 1$  **do**
- 4:      $\beta'_i = (L + U)/2$
- 5:      $n'_{b_i} = \lceil \beta'_i n_{b_i} \rceil$ , retrain CNN
- 6:     **if** Accuracy distortion  $< \delta$  **then**
- 7:        $U = \beta'_i$
- 8:     **else**
- 9:        $L = \beta'_i$
- 10:    **end if**
- 11:    **end while**
- 12:     $\beta_i = \beta'_i$
- 13: **end for**
- 14: **return**  $\beta = [\beta_0, \beta_1, \dots, \beta_m]$

---

Our algorithm BRIEF retrains the CNN from scratch (step 5) to investigate the prediction accuracy of current configuration since our lesion studies have demonstrated network robustness against channel removal. The retraining process can be relaxed by fewer training epochs as long as the training setting can retain the original CNN prediction accuracy. Once the accuracy distortion is acquired, we can adjust the upper bound and the lower bound for  $\beta_i$  accordingly using a greedy binary search method (steps 7 and 9).

Earlier we mentioned that to ensure information being sufficiently maintained for the classification task, which is performed at the last layer of a CNN, we propose performing backward reduction. To confirm this backward heuristic to be accurate, we conducted experiments to compare the effectiveness of backward versus forward reduction. Table II shows that backward reduction outperforms forward reduction significantly in size (45.3% versus 6.3%) at a similar predic-

TABLE II

PERFORMANCE COMPARISON BETWEEN THE FORWARD REDUCTION (REDUCTION SEQUENCE  $[b_0, b_1, b_2]$ ) AND THE BACKWARD REDUCTION (REDUCTION SEQUENCE  $[b_2, b_1, b_0]$ ) FOR THE SEQUENTIAL CNN WITH CONVOLUTION DEPTH = 15 ON CIFAR-10.

Model	Acc. (%) [Diff.]	Size (MB)	Saving (%)
Original	91.24	0.87	-
Forward	90.46 [0.78]	0.82	6.3
Backward	90.31 [0.93]	0.48	<b>45.3</b>

tion accuracy. As a result, the backward reduction algorithm acts to remove the channels with low information density. Therefore, the network can recover information loss from the latter macroblocks when there is sufficient information provided from the earlier macroblocks. On the other hand, the forward reduction approach removes information starting from the input source, which distorts the original information and eliminates the network’s ability to recover from such distortion.

#### IV. EXPERIMENTAL RESULTS

This section reports experimental results with BRIEF on the ImageNet dataset for various CNN models. We conducted BRIEF’s backward reduction algorithm on the last two convolution macroblocks. We implemented BRIEF with PyTorch 0.3. Our evaluation metric is model size. (We care about model compaction not to significantly degrade prediction accuracy, but we do not compare accuracy between different CNN models.) To realistically measure model size, we use the actual required storage (including headers) of a trained model (i.e., `state_dic` in PyTorch).

##### A. ImageNet Dataset

ImageNet consists of 1.28M training images and 50k validation images, divided into 1,000 classes. We trained our models for 90 epochs with a batch size of 256. The learning rate, set to 0.1 initially, is divided by 10 at epoch 30 and 60. Simple data augmentation was adopted based on the ImageNet script by PyTorch, which is the same as [5]. The single-center-crop validation accuracy is reported for the CNN models.

In order to reduce the computational effort of BRIEF’s greedy backward reduction process on ImageNet, we empirically adopted the shorter training setting of 20 training epochs with a learning rate (set to 0.1 initially) divided by 10 at epoch 8 and 16. We used 20-epoch setting in Algorithm 1 to quickly find the best  $\beta$ , and eventually used this  $\beta$  to train the final model for 90 epochs. Then, we evaluated the final performance by training the CNN in the original 90-epoch training setting.

For the shorter training setting, we designed and performed experiments to determine training epochs. In these experiments, we trained several CNN models for different training epochs and fixed the other hyper-parameters of the training. The different choices of training epochs we explored are 10, 20 and 30. We observed that 1) there is considerable discrepancy

TABLE III

PERFORMANCE COMPARISON BETWEEN OUR METHOD AND THE PREVIOUS WORK OF RESNET-34 ON IMAGENET.

ResNet-34	Top-1 (%)	Param. ( $10^7$ )	Saving
Baseline of [7]	73.23	2.16	-
[7]	72.17 [1.06]	1.93	10.8%
Baseline	<b>73.54</b>	2.18	-
Proposed	<b>72.49 [1.05]</b>	<b>1.48</b>	<b>32.3%</b>

between the results of 10-epoch and 90-epoch settings, 2) the results of 20-epoch setting can most reflect the results of 90-epoch setting, and 3) the results of 20-epoch and 30-epoch settings are basically the same. Based on these three observations of our designed experiments, we thus selected 20 as our shorter training setting.

##### B. Evaluation of Various CNN Models

Table III reports that BRIEF significantly outperforms the state-of-the-art approach [7] conducted on ResNet-34, a convolution-layer dominant CNN model. BRIEF reduces the model by  $3\times$  more (32.8%) than the previous work does (10.8%) with similar top-1 accuracy. Our algorithm removed the channels aggressively even including the non-zero weighting parameter as long as the prediction accuracy is maintained. Therefore, we can explore the additional regions that are ignored by the traditional approaches. This result confirms the great potential in model reduction from the perspective on information flow.

We evaluated our method on a variety of Convolution-layer dominant CNN models (e.g., ResNet, MobileNet, and SqueezeNet) since these compact models are more challenging targets. MobileNet is a tough reduction target because it has a width-multiplier technique that adjusts all the channel numbers by the same scaling factor. We also evaluated the proposed backward reduction method on the further scaling-reduced MobileNets (e.g., 0.5-MobileNet). We reported the scaling factors for the final two macroblocks of SqueezeNet with irregular structure and the actual channel number in the experiments for the CNNs with regular structures.

Table IV presents the performance of BRIEF among the various Convolution-layer dominant CNN models. The configuration column of Table IV shows the architecture of each convolution macroblock before and after the proposed backward reduction algorithm. The accuracies of the CNN models in Table IV are evaluated using the 90-epoch training setting. We achieved an up to 37.56% model size reduction on MobileNet with only a 0.56% accuracy loss.

Notice that the model reduction ratio decreases as we applied BRIEF on the further optimized MobileNets (e.g., 0.75-MobileNet, 0.5-MobileNet). Even for 0.5-MobileNet, we still accomplished a 29.3% model size reduction, which resulted in a storage size of only 3.63 MB. The model size of the reduced 0.5-MobileNet (3.63 MB) is already smaller than that of SqueezeNet (4.72 MB), while the prediction accuracy

TABLE IV  
 BACKWARD REDUCTION RESULTS FOR THE CNN MODELS. THE CONFIGURATION SHOWS THE CHANNELS NUMBERS OF THE LAST TWO CONVOLUTION MACROBLOCKS. WE REPORT THE SCALING FACTORS FOR SQUEEZE NET DUE TO THE IRREGULAR STRUCTURE.

Model	Top-5 (%) [Diff.]	Param. ( $10^6$ )	Size (MB)	Saving (%)	Config.
ResNet-34	91.410	21.80	83.24	-	[256, 512]
Proposed	90.854 [0.556]	14.80	56.52	<b>32.10</b>	[256, 346]
ResNet-18	89.350	11.69	44.64	-	[256, 512]
Proposed	88.866 [0.484]	8.45	32.28	<b>27.69</b>	[245, 405]
1.0-MobileNet	88.520	4.23	16.25	-	[512, 1024]
Proposed	87.952 [0.568]	2.64	10.15	<b>37.56</b>	[507, 513]
0.75-MobileNet	86.992	2.59	9.95	-	[384, 768]
Proposed	86.500 [0.492]	1.67	6.44	<b>35.28</b>	[369, 442]
0.5-MobileNet	83.972	1.33	5.14	-	[256, 512]
Proposed	82.792 [1.180]	0.94	3.63	<b>29.31</b>	[252, 331]
SqueezeNet 1.1	79.220	1.24	4.72	-	$\beta = [1.0, 1.0]$
Proposed	78.602 [0.618]	1.10	4.21	<b>10.81</b>	$\beta = [0.8, 0.9]$



Fig. 7. Rate-Distortion curve of the scaling-only and the scaling with backward reduction approaches.

of MobileNet still outperforms SqueezeNet. For the highly optimized CNN, SqueezeNet, we achieved a 10.81% model reduction while the accuracy loss remains within 1%.

### C. Rate-Distortion Behavior

We compared our backward reduction algorithm to the traditional  $\alpha$ -scaling approach that multiplies the whole CNN to the same scaling factor  $\alpha$ . The configuration is set to  $\mathbf{n}_b = [32, 64, 128]$  for the sequential CNN on CIFAR-100 in this experiment. Figure 7 shows the RD curves of the scaling-only approach and the scaling with our backward reduction algorithm. The scaling factor  $\alpha$  ranges from 0.5 to 0.9 with step size 0.1. The  $x$ -axis represents the required bit rate (KB), and the  $y$ -axis denotes the prediction accuracy. The RD performance experiment is conducted on the sequential CNN with convolution depth = 12. For the vast majority of models, the  $\alpha$ -scaling with BRIEF further improves the simple  $\alpha$ -scaling approach in terms of RD performance.

## V. CONCLUSION

The conjectured information flow structure describes CNNs as dynamic structures rather than static ones. As long as sufficient information is provided from the prior convolution macroblocks, we can safely remove the redundant channels and still maintain the same level of accuracy. Therefore, we can explore the additional regions of CNNs, which were not possible with the traditional filter magnitude based approaches. Using our backward reduction algorithm BRIEF, we reduced ResNet-34 significantly, attaining  $3\times$  better reduction than previous approaches. We also reduced MobileNet to just 3.63 MB, making it smaller than SqueezeNet (4.72 MB), while achieving a slightly higher prediction accuracy. The capability of backward reduction was validated on highly compact CNNs, including SqueezeNet and MobileNet.

Our method is applied at the macroblock level, which the greedy algorithm may impose the computational burden for searching the proper channel number for the macroblock. We plan to derive the minimum required channel number directly with the aid of further information flow analysis for model reduction in our future work. The proposed greedy algorithm demonstrates the potential of model reduction by leveraging the information flow analysis, which we expect this work to act as a stepping stone towards opening the black-box of CNNs to establish more efficient and compact CNN models. Our macroblock level model reduction method complements to the reduction approaches conducted in the fine-grained level (e.g., sparse filter connection), which will achieve a compound improvement in model compression.

## REFERENCES

- [1] A. Romero, N. Ballas, S. E. Kahou, A. Chassang, C. Gatta, and Y. Bengio, "Fitnets: Hints for thin deep nets," *International Conference on Learning Representations (ICLR)*, 2015.



- [2] G. Hinton, O. Vinyals, and J. Dean, “Distilling the knowledge in a neural network,” in *Deep Learning and Representation Learning Workshop, NIPS*, 2014.
- [3] R. Shwartz-Ziv and N. Tishby, “Opening the black box of deep neural networks via information,” *CoRR*, vol. abs/1703.00810, 2017.
- [4] A. G. Howard, M. Zhu, B. Chen, D. Kalenichenko, W. Wang, T. Weyand, M. Andreetto, and H. Adam, “Mobilenets: Efficient convolutional neural networks for mobile vision applications,” *CoRR*, vol. abs/1704.04861, 2017.
- [5] K. He, X. Zhang, S. Ren, and J. Sun, “Deep residual learning for image recognition,” in *IEEE Conference on Computer Vision and Pattern Recognition (CVPR)*, June 2016.
- [6] F. N. Iandola, M. W. Moskewicz, K. Ashraf, S. Han, W. J. Dally, and K. Keutzer, “Squeezenet: Alexnet-level accuracy with 50x fewer parameters and <1mb model size,” *CoRR*, vol. abs/1602.07360, 2016.
- [7] H. Li, A. Kadav, I. Durdanovic, H. Samet, and H. P. Graf, “Pruning filters for efficient convnets,” *International Conference on Learning Representations (ICLR)*, 2017.
- [8] G. Huang, Z. Liu, L. van der Maaten, and K. Q. Weinberger, “Densely connected convolutional networks,” in *CVPR*, July 2017.
- [9] S. Ioffe and C. Szegedy, “Batch normalization: Accelerating deep network training by reducing internal covariate shift,” in *International Conference on Machine Learning (ICML)*, vol. 37. Lille, France: PMLR, 07–09 Jul 2015, pp. 448–456.
- [10] C. Szegedy, V. Vanhoucke, S. Ioffe, J. Shlens, and Z. Wojna, “Rethinking the inception architecture for computer vision,” in *IEEE Conference on Computer Vision and Pattern Recognition (CVPR)*, June 2016.
- [11] A. Krizhevsky, I. Sutskever, and G. E. Hinton, “Imagenet classification with deep convolutional neural networks,” in *International Conference on Neural Information Processing Systems (NIPS)*, ser. NIPS’12, 2012, pp. 1097–1105.
- [12] K. Simonyan and A. Zisserman, “Very deep convolutional networks for large-scale image recognition,” *CoRR*, vol. abs/1409.1556, 2014.
- [13] V. Sze, Y. H. Chen, T. J. Yang, and J. S. Emer, “Efficient processing of deep neural networks: A tutorial and survey,” *Proceedings of the IEEE*, vol. 105, no. 12, pp. 2295–2329, Dec 2017.
- [14] B. Liu, M. Wang, H. Foroosh, M. Tappen, and M. Pensky, “Sparse convolutional neural networks,” in *IEEE Conference on Computer Vision and Pattern Recognition (CVPR)*, June 2015.
- [15] S. Han, H. Mao, and W. J. Dally, “Deep compression: Compressing deep neural networks with pruning, trained quantization and huffman coding,” *International Conference on Learning Representations (ICLR)*, 2016.
- [16] S. Han, X. Liu, H. Mao, J. Pu, A. Pedram, M. A. Horowitz, and W. J. Dally, “Eie: Efficient inference engine on compressed deep neural network,” *International Symposium on Computer Architecture (ISCA)*, 2016.
- [17] A. Aghasi, A. Abdi, N. Nguyen, and J. Romberg, “Nettrim: Convex pruning of deep neural networks with performance guarantee,” in *International Conference on Neural Information Processing Systems (NIPS)*, 2017, pp. 3180–3189.
- [18] I. Hubara, M. Courbariaux, D. Soudry, R. El-Yaniv, and Y. Bengio, “Binarized neural networks,” in *International Conference on Neural Information Processing Systems (NIPS)*, 2016, pp. 4107–4115.
- [19] M. Rastegari, V. Ordonez, J. Redmon, and A. Farhadi, “Xnor-net: Imagenet classification using binary convolutional neural networks,” in *European Conference on Computer Vision (ECCV)*, 2016, pp. 525–542.
- [20] J. Wu, C. Leng, Y. Wang, Q. Hu, and J. Cheng, “Quantized convolutional neural networks for mobile devices,” in *IEEE Conference on Computer Vision and Pattern Recognition (CVPR)*, June 2016.
- [21] S. Gupta, A. Agrawal, K. Gopalakrishnan, and P. Narayanan, “Deep learning with limited numerical precision,” in *International Conference on Machine Learning (ICML)*, vol. 37. Lille, France: PMLR, 07–09 Jul 2015, pp. 1737–1746.
- [22] W. Tang, G. Hua, and L. Wang, “How to train a compact binary neural network with high accuracy?” in *Association for the Advancement of Artificial Intelligence (AAAI)*, 2017.
- [23] X. Lin, C. Zhao, and W. Pan, “Towards accurate binary convolutional neural network,” in *International Conference on Neural Information Processing Systems (NIPS)*, 2017, pp. 344–352.
- [24] Z. Liu, J. Li, Z. Shen, G. Huang, S. Yan, and C. Zhang, “Learning efficient convolutional networks through network slimming,” in *IEEE International Conference on Computer Vision (ICCV)*, Oct 2017.
- [25] Y. He, X. Zhang, and J. Sun, “Channel pruning for accelerating very deep neural networks,” in *IEEE International Conference on Computer Vision (ICCV)*, Oct 2017.
- [26] A. Veit, M. Wilber, and S. Belongie, “Residual networks behave like ensembles of relatively shallow networks,” in *International Conference on Neural Information Processing Systems (NIPS)*, 2016, pp. 550–558.
- [27] T. M. Cover and J. A. Thomas, *Elements of Information Theory*. Wiley-Interscience, 2006.
- [28] B. Zoph, V. Vasudevan, J. Shlens, and Q. V. Le, “Learning transferable architectures for scalable image recognition,” *CoRR*, vol. abs/1707.07012, 2017.